

# EFFECTS OF TEMPERATURE AND PRESSURE ON THE STRUCTURE OF FGD SCRUBBER SLUDGE

S. P. Kelley<sup>1</sup>, P. S. Valimbe<sup>1</sup>, V. M. Malhotra<sup>1</sup>, and D. D. Banerjee<sup>2</sup>

(1) Department of Physics, Southern Illinois University, Carbondale, IL 62901

(2) Illinois Clean Coal Institute, Carterville, IL 62918.

## ABSTRACT

Approximately 20 million tons of flue gas desulfurization (FGD) residue are generated in the US every year. To find cost effective disposal approaches for FGD residue, we are attempting to fabricate composite materials from the sludges. We subjected the as-received scrubber sludge (CWLP, Springfield, Illinois) and the sludge which had been dried at 180°C to various formation pressures and temperatures to form 3.2 and 5.7 cm diameter cylinders. The chemical and physical structures of the pressurized materials were probed using scanning electron microscopy (SEM), transmission-Fourier transform infrared (FTIR), and differential scanning calorimetry (DSC) techniques. The formation temperature ( $20^{\circ}\text{C} < T < 220^{\circ}\text{C}$ ) and pressure ( $400 \text{ psi} < P < 5500 \text{ psi}$ ) were variables. The formation pressure did not affect the crystal growth habits of the materials. However, the formation temperature not only controlled the size of the crystallites in our materials, but it also influenced the chemical structure of the fabricated materials.

## INTRODUCTION

In the past when electric power utilities shifted from oil to coal for electric power generation, it created environmental concerns related to the emission of  $\text{SO}_x$  and  $\text{NO}_x$  from the combustion of coal [1]. These gases are formed in combustion units due to oxidation of sulfur and nitrogen present in coal. To mitigate environmental concerns, various technologies have been developed including Flue Gas Desulfurization (FGD). FGD technology involves the use of scrubbers which utilize lime or limestone to capture the flue gases. Unfortunately, though FGD technology is successful in reducing the emission of undesirable gases, it generates a large quantity of solid waste in the form of scrubber sludge. In fact, approximately 20 million tons of FGD residues are generated annually in the United States. The properties of these solid wastes strongly depend on the type of coal used in the combustion units as well as the desulfurization process employed [2]. In general, the scrubber sludge is believed to contain mostly gypsum ( $\text{CaSO}_4 \cdot 2\text{H}_2\text{O}$ ), calcium sulfate ( $\text{CaSO}_4$ ), calcium sulfite ( $\text{CaSO}_3$ ), calcite ( $\text{CaCO}_3$ ), and in addition small quantities of fly ash and excess reagents [3,4]. Of the different types, wet scrubber units are the most commonly used for  $\text{SO}_2$  removal from flue gases. The purity of gypsum obtained from a wet scrubber unit is believed to range from 95% to 99%.

The disposal of 20 million tons of scrubber sludge annually is in itself becoming a serious economic problem for coal utilities. Even though different usages of scrubber sludges have been proposed in road base construction [5,6], prefabricated products (gypsum boards) [7], the cement industry [5,7], plaster fabrication [7], and agriculture [7,8], their overall utilization is still very small. This is largely due to the changes in the sludges' properties from batch to batch and unit to unit as well as to market specifications and seasonal variations. Unfortunately, a major portion of the total amount of scrubber sludge generated continues to be dumped in landfills.

The implementation of the Clean Air Act of 1990 will require new utilization of scrubber sludges. Proposed applications of synthetic gypsum, produced by certain power plants, are the formation of plaster [7], formation of binder material, self leveling floor screeds, and fiber reinforced slabs from FGD sludge [9]. In addition, we have been exploring techniques of forming structural composite materials from both sulfate- and sulfite-rich FGD sludges. Before these technologies can be matured, we must understand how formation pressure and temperature affect the crystalline growth habits of the sludge and how these parameters affect the structure of the formed material. Therefore, we subjected a sulfate-rich scrubber sludge to various structural formation conditions and examined the formed materials with the help of SEM, DSC, and FTIR techniques.

## EXPERIMENTAL TECHNIQUES

The present study is based on materials fabricated from a scrubber sludge generated by the City Water and Light Power plant (CWLP) in Springfield, Illinois. The scrubber sludge sample was obtained from the sample bank maintained by the Department of Mining Engineering at Southern Illinois University, Carbondale, Illinois. The as-received sample was in a thick slurry form, and

the sample was air dried at room temperature prior to fabricating materials from it. Our characterization studies showed this material to be largely  $\text{CaSO}_4 \cdot 2\text{H}_2\text{O}$  [10].

The cylindrical disks of the material were formed by hot pressing the CWLP scrubber sludge in dies of diameter 3.2 cm and 5.7 cm, respectively. The length of the cylinders varied from 2.5 cm to 7.5 cm. We used temperature ( $20^\circ\text{C} < T < 220^\circ\text{C}$ ), pressure ( $400 \text{ psi} < P < 5000 \text{ psi}$ ), and hot pressing time ( $15 \text{ min.} < T < 120 \text{ min.}$ ) as variables in forming the materials. We fabricated our disks using two different methods. In the first, the air dried samples were used with water to form a slurry paste, which was subjected to the conditions mentioned above. In the second approach, the CWLP scrubber sludge was thermally treated in air at  $180^\circ\text{C}$  for two hours to convert the sludge into hemihydrate ( $\text{CaSO}_4 \cdot 0.5\text{H}_2\text{O}$ ) crystals. This white powdery material was then combined with water to form a slurry [11] which was subsequently used to form the cylinders as described above. The formation parameter summary and identification of the samples are listed in Table 1.

Table 1  
The sample identity and formation conditions of cylindrical disks.

Sample Identity	Formation Conditions		
	Time (minutes)	Pressure (psi)	Temperature ( $^\circ\text{C}$ )
CWLP A1	20	5,000	24
CWLP A2	20	4,000	24
CWLP A3	20	3,000	24
CWLP A4	20	2,000	24
CWLP B1	20	4,000	60
CWLP B2	20	4,000	100
CWLP B3	20	4,000	140
CWLP B4	20	4,000	180
SPK 31	90	2,500	94
SPK 32	90	2,500	125
SPK 29	90	2,500	200
SPK 33	90	500	160
SPK 34	90	1,500	160
SPK 35	90	4,500	160

The morphology of the crystallites formed in our cylinders was studied using a Hitachi S570 scanning electron microscope. Initially, we cut small pieces of the cylinder with the help of a diamond saw. However, our SEM results exhibited smooth surface textures of the cut material, clearly indicating that the sawing itself affected the crystallites. Therefore, the samples were prepared by breaking the cylinders and extracting small pieces of the material from the interior as well as from the exterior of the cylinders. The pieces were mounted on the SEM sample stubs, using carbon paint, and were placed in an oven at  $60^\circ\text{C}$  for 24 hours to allow their fixation on the stubs. The samples, thus mounted, were sputter coated with a 40 nm of Ag/Pd layer to avoid the problem of charging. The SEM study was carried out using an accelerating voltage of 20 kV.

The thermal behavior of the fabricated materials, i.e., CWLP Ax ( $x = 1, 2, 3$  or 4), CWLP Bx ( $x = 1, 2, 3$ , or 4), and SPKxx ( $xx = 29, 31, 32, 33, 34$ , or 35) was recorded using a Perkin-Elmer DSC7 system [12, 13]. To record the DSC thermographs at  $40^\circ\text{C} < T < 300^\circ\text{C}$ , the samples were sealed in aluminum pans with a hole drilled in them so that gases or vapors could escape easily. The transmission-FTIR data were collected using a nujol mull technique. Thin films of nujol mull, containing the ground sample, were formed on the KBr windows. The FTIR spectra of the various samples were recorded at  $4 \text{ cm}^{-1}$  resolution using an IBM IR44 FTIR spectrometer.

## RESULTS AND DISCUSSION

**Microscopic Results:** The CWLP Ax series was formed with a view to explore how pressure affects the crystal growth habit of sludge-derived hemihydrate powder at room temperature.

Figure 1 reproduces the microphotograph of CWLP A1 sample. The SEM pictures revealed that for all CWLP Ax series the crystals were mostly needle-shaped with thin needles ranging from 2.5  $\mu\text{m}$  to 40  $\mu\text{m}$  in length. However, most of the crystals were around 2.5  $\mu\text{m}$  in length. On average the thickness of the needles was about 2.5  $\mu\text{m}$ . A similar compact, needle-shaped crystal growth habit has been reported for hydrated calcium sulfate when hemihydrate crystals were exposed to water vapor [14]. We did not observe any effect of pressure on the growth habit of crystallites for CWLP Ax series.

The effect of temperature on the crystallization behavior of hemihydrate was studied by fabricating CWLP Bx series in which a hemihydrate-water slurry was hot pressed at  $50^\circ\text{C} < T < 200^\circ\text{C}$  at a constant pressure of 4000 psi. Similar to the results of CWLP Ax series, CWLP B1 sample also showed small needle-shaped crystals of gypsum. This sample was fabricated at  $60^\circ\text{C}$ . As the fabrication temperature increased, the size of crystallites formed in the sample also increased. This can be clearly seen in Fig. 2 which depicts the SEM photograph of CWLP B4 sample grown at  $180^\circ\text{C}$ . SEM pictures of CWLP B2 fabricated at  $100^\circ\text{C}$  showed a few small parallelogram-shaped crystals (length  $\sim 18$   $\mu\text{m}$ , thickness  $\sim 3$   $\mu\text{m}$ ) in addition to mostly needle-shaped crystals. The parallelogram-shaped crystals are a typical morphology for gypsum [10]. On increasing the formation temperature to  $140^\circ\text{C}$  and  $180^\circ\text{C}$ , we observed not only the increase in the size of crystals formed but interestingly also the cession of needle-shaped crystals. Large interlocked crystals over the range from 20  $\mu\text{m}$  to 240  $\mu\text{m}$  in length and of thicknesses varying from 5  $\mu\text{m}$  to 50  $\mu\text{m}$  were formed at  $180^\circ\text{C}$ . It appears from our results that while formation pressure has only a marginal effect on the crystal growth habit, the formation temperature drastically alters the crystal growth behavior of sludge-derived hemihydrate.

In the second set of experiments, we examined how pressure and temperature affected the crystal growth habits of as-received scrubber sludge, i.e., gypsum-water slurry. Unlike previously discussed results, where we converted the sludge into hemihydrate powder by heating the sludge at  $180^\circ\text{C}$  (CWLP Ax and CWLP Bx series), in the present set of experiments (SPKxx series) the sludge was only air dried at room temperature prior to forming the materials. Figure 3 shows SEM microphotograph of SPK31 sample, which clearly shows large crystals are formed ranging from 6  $\mu\text{m}$  to 50  $\mu\text{m}$  in length, while the thickness varied from 2  $\mu\text{m}$  to 20  $\mu\text{m}$ . A comparison of these dimensions with those of CWLP B2 led us to conclude that the starting phase of the hydrated calcium sulfate influences the size and morphology of the crystals formed at  $T < 140^\circ\text{C}$ . On increasing the formation temperature to  $125^\circ\text{C}$  (SPK32 sample), a further increase in the dimensions of the crystals resulted. For SPK31 particle size ranged from 8  $\mu\text{m}$  to more than 100  $\mu\text{m}$  in lengths and thickness varied from 8  $\mu\text{m}$  to 30  $\mu\text{m}$ . However, an increase in temperature to  $200^\circ\text{C}$  revealed that crystals started to form which resembled needle-like shapes and the crystallites were compacted in the sample.

The SPK33, SPK34, and SPK35 samples were formed at a fixed temperature of  $160^\circ\text{C}$  using different pressures. A comparative analysis of SEM pictures of SPK33 and SPK 35 showed that while the surfaces of the crystallites in SPK35 (formed at 4500 psi) had considerable roughness and flaky-like appearance, this was not the case for SPK33 which was formed at a much lower pressure, i.e., 500 psi. Since both samples were fabricated by hot pressing the slurry at the same temperature for equal lengths of time, it was possible that the surface roughness observed for SPK35 sample was the consequence of higher pressure used. One possible explanation could be that these flaky structures were formed by escaping water molecules, thus leaving traces of "water channels". These traces were oriented in one particular direction, i.e., in the longitudinal direction of the crystallites. Since under our hot pressing conditions, the water vapors could only escape from the rim of our die, therefore, it was not surprising to observe oriented defects on the surface of the crystallites. The crystal dimensions were not affected by the pressure applied like for CWLP Ax series, and in general crystallite sizes varied from 10  $\mu\text{m}$  to 90  $\mu\text{m}$  in length and 4  $\mu\text{m}$  to 30  $\mu\text{m}$  in thickness.

**Thermal and Infrared Results:** It is well known [10,15,16] that gypsum undergoes a two step dehydration process at  $110^\circ\text{C} < T < 220^\circ\text{C}$ . Therefore, DSC experiments could be used to identify the phases of the calcium sulfate formed in our materials. For example, Fig. 4 reproduces the observed DSC thermographs of SPK29 and SPK31 samples formed at 2500 psi pressure at  $94^\circ\text{C}$  and  $200^\circ\text{C}$ , respectively. Two endothermic peaks were observed for SPK31 sample at around  $170^\circ\text{C}$  and  $195^\circ\text{C}$ , while a single endothermic peak was seen for SPK29 sample at around  $195^\circ\text{C}$ . In our thermal characterization measurements on CWLP scrubber sludge [10], we observed two endothermic peaks centered at around  $154^\circ\text{C}$  and  $189^\circ\text{C}$ . The first endothermic peak was associated with  $\text{CaSO}_4 \cdot 2\text{H}_2\text{O}$  decomposing into  $\text{CaSO}_4 \cdot 0.5\text{H}_2\text{O}$  and the second endothermic peak with the dehydration of  $\text{CaSO}_4 \cdot 0.5\text{H}_2\text{O}$  into  $\text{CaSO}_4$ . The shift in the peak temperatures seen for SPK31 sample could be attributed to the compaction of the crystallites,

presenting additional mechanical barriers for water's desorption. Thus, shifts in the temperatures of endothermic peaks were produced. It is therefore argued that while SPK31 sample crystallized perhaps in gypsum phase, the crystallites formed in SPK29 sample were hemihydrate. All the samples fabricated in CWLP Ax and CWLP Bx series exhibited a two-step dehydration endothermic reaction. This result leads us to believe that the gypsum crystallites were present in all these fabricated samples. Whether hemihydrate phase was also present can not be answered from DSC measurements alone since the presence of both gypsum and hemihydrate phases in the sample will still generate two endothermic reactions. However, it is possible for us to argue that only hemihydrate phase was formed for SPK29, SPK33, SPK34, and SPK35 samples since we observed a single endothermic reaction at around 190°C.

Infrared spectroscopic technique [10,17] can be used to further verify and identify which calcium sulfate phases have formed in our fabricated cylinders. In water's stretching region, gypsum produces three vibrational modes at around 3550, 3490 (weak band), and 3400  $\text{cm}^{-1}$ ; while in the bending region, two distinct oscillators are observed at 1686 and 1623  $\text{cm}^{-1}$ . For hemihydrate structure, two vibrational bands in the stretching region appear at around 3610 and 3555  $\text{cm}^{-1}$ . A single vibrational mode is seen at around 1620  $\text{cm}^{-1}$  for the hemihydrate in the bending region. If anhydrous calcium sulfate phase is present, then that phase will produce no water bands but still can be recognized from  $\text{SO}_4^{2-}$  ions' vibrations. We have summarized our FTIR results for CWLP Ax, CWLP Bx, and SPKxx series in Table 2. The identified phases are also listed in that table. The CWLP Ax and CWLP Bx ( $x = 1,2$ ) cylinders were largely composed of gypsum crystallites with some hemihydrate crystallites also present. The CWLP Bx ( $x = 3, 4$ ) cylinders on the other hand were formed from largely hemihydrate crystallites with some gypsum phase also present in them. It is interesting to note that if as-received, but air dried, CWLP scrubber sludge was used to fabricate the materials then the cylinders, depending upon formation temperature, either crystallized in gypsum or hemihydrate phase rather than in mixed phases like CWLP Ax and CWLP Bx series.

#### ACKNOWLEDGMENTS

This work was supported in part by Illinois Clean Coal Institute (Illinois Department of Commerce and Community Affairs).

#### REFERENCES:

1. Randolph, A. D.; Kelly, B. J.; Keough, B. "Calcium Sulfite and Calcium Sulfate Crystallization, Vol.1: Effect of Crystallization Type on Gypsum Size Distribution", *EPRI, Palo Alto, California, Research Project 1031-3*, Nov. 1986.
2. Puri, V.K.; Paul, B. C.; Mukherjee, J.; Hock, K. K.; Yu, Z. "Utilization Coal Refuse and FBC Fly Ash: Strength Aspects", *Procd. NMLRC Sympos. (Eds.) Y. P. Chugh and D. C. Davin*, pp 187-195, 1993.
3. Clarke, L. B. "Management of FGD residues: An International Overview", *Procd. 10th Pittsburgh Coal Conf., (Ed.) S-H Chiang*, pp. 561-566, 1993.
4. Taulbee, D. N.; Graham, U.; Rathbone, R. F.; Robl, T. L. *Am. Chem. Soc. Prep., Div. Fuel Chem. 40(4)*, 858, 1995.
5. Valimbe, P. S.; Malhotra, V. M.; Banerjee, D. D.; *Am. Chem. Soc. Prep., Div. Fuel Chem., 40(4)*, 776, 1995.
6. Goodrich-Mahoney, J. W. "Coal Combustion By-products Field Research Program at EPRI: An Overview", *EPRI (Environmental Division)*, 1994.
7. Luckevich, L. M. "Making and Marketing Flue Gas Desulfurization Gypsum", *Procd. 12th Inter. Sympos. on Coal Combustion By-Products Management and Use, Orlando, Florida, Vol. 2*, pp 67-1 to 67-7, 1997.
8. Chou, M.-I. M.; Bruinius, J. A.; Li, Y. C.; Rostam-Abadi, M.; Lytle, J. M. *Am. Chem. Soc. Prep., Div. Fuel Chem. 40(4)*, 896, 1995.
9. Schlieper, H.; Duda, A.; Jager, R.; Kanig, M.; Kwasny-Echterhagen, R. "FGD Gypsum - A Raw Material for New Binder Systems" *Procd. 12th Inter. Sympos. on Coal Combustion By-Products Management and Use, Orlando, Florida, Vol. 2*, pp 48-1 to 48-13, 1997.
10. Valimbe, P. S.; Malhotra, V. M.; Banerjee, D. D.; *Am. Chem. Soc. Prep., Div. Fuel Chem., 1997 (this volume)*.
11. Lynch, W. M. *Am. Ceramic Soc. Bull.* 74, 60, 1995.
12. Jasty, S.; Malhotra, V. M. *Phys. Rev. B* 45, 1, 1992.
13. Jasty, S.; Malhotra, V. M.; Robinson, P. D. *J. Physics: Condens. Matter* 4, 4769, 1992.
14. Gans, W.; Klocker, H.; Knacke, O. Z. *Metallkd.* 87, 98, 1996.
15. Blaine, R. *American Laboratory, Sept. 1995*, pp 24-28.

16. Dunn, J. G.; Oliver, K.; Sills, I. *Thermochim. Acta* **155**, 93, 1989.  
 17. Bensted, J.; Prakash, S. *Nature* **219**, 60, 1968.

Table 2

The observed water bands for various samples fabricated from CWLP scrubber sludge and the possible crystallite phases. CWLP HP represents hemihydrate phase derived from the sludge by heating it at ambient pressure at 180°C.

Sample Name	Water Stretching Vibrations (cm <sup>-1</sup> )	Water Bending Band (cm <sup>-1</sup> )	Phase Identified
CWLP HP	3607, 3553, 3406	1622	Largely Hemihydrate
CWLP A4	3607, 3551, 3404	1685, 1622	Gypsum + Hemihydrate
CWLP A1	3608, 3553, 3404	1685, 1622	Gypsum + Hemihydrate
CWLP B1	3607, 3545, 3400	1686, 1620	Gypsum + Hemihydrate
CWLP B2	3607, 3553, 3404	1686, 1620	Gypsum + Hemihydrate
CWLP B3	3609, 3553, 3404	1685, 1620	Hemihydrate + Gypsum
CWLP B4	3607, 3553, 3404	1685, 1620	Hemihydrate + Gypsum
SPK 31	3543, 3493, 3400	1688, 1622	Gypsum
SPK 32	3545, 3493, 3400	1685, 1622	Gypsum
SPK 29	3609, 3555	1618	Hemihydrate
SPK 33	3611, 3555	1621	Hemihydrate
SPK 35	3611, 3555	1620	Hemihydrate

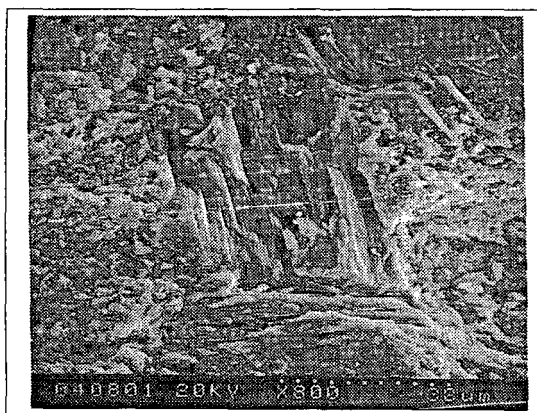


Figure 1. SEM microphotograph of sample fabricated from hemihydrate powder derived from CWLP scrubber sludge. The water slurry was pressed at 5000 psi pressure for 20 minutes at 24°C.

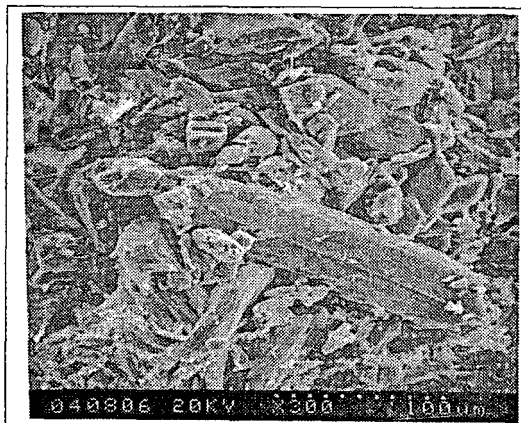


Figure 2. SEM microphotograph of sample fabricated from hemihydrate powder derived from CWLP scrubber sludge. The water slurry was pressed at 4000 psi pressure for 20 minutes at 180°C.

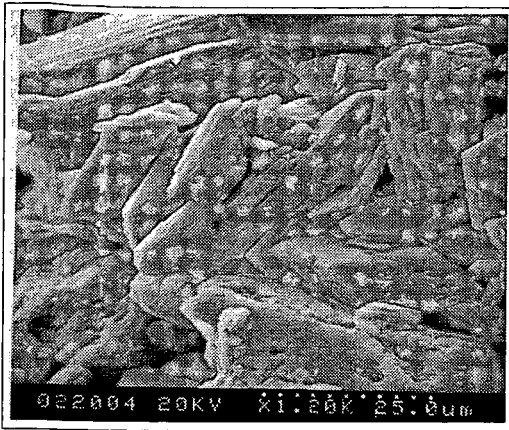


Figure 3. SEM microphotograph of sample fabricated from CWLP scrubber sludge. The water slurry was pressed at 2500 psi pressure for 90 minutes at 94°C.

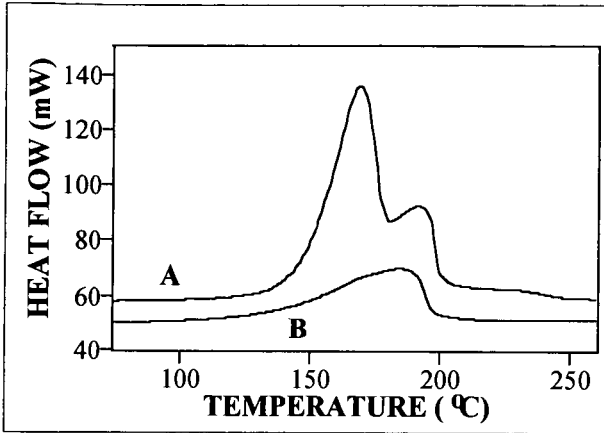


Figure 4. The observed DSC thermographs for (A) SPK31 sample formed at 94°C at 2500 psi pressure and (B) SPK29 sample fabricated at 200°C at 2500 psi pressure.

